Paleomagnetism and kinematics of the central Olyutorsky Range, Koryak Highland

Article *in* Geotectonics · March 1996

CITATIONS
7

READS
17

1 author:

Dmitry Viatcheslavovich Kovalenko
Russian Academy of Sciences
85 PUBLICATIONS **227** CITATIONS

SEE PROFILE

Geotectonics, Vol. 30, No. 3, 1996, pp. 243–257. Translated from Geotektonika, No. 3, 1996, pp. 82–96.

Paleomagnetism and Kinematics of the Central Olyutorsky Range, Koryak Highland

D. V. Kovalenko

Institute of the Lithosphere, Russian Academy of Sciences, Staromonetnyi per. 22, Moscow, 109180 Russia

Received June 6, 1994

Abstract—New paleomagnetic data for the Olyutorsky Range, Koryak Highland, were obtained. The paleolatitudes, calculated for the Late Cretaceous island-arc complexes, fall approximately into an interval near 50°N. The island-arc complexes studied cannot be properly aligned with either Eurasia, or North America at a time close to the Cretaceous–Paleogene boundary. The island-arc and oceanic strata were rotated clockwise around the vertical axis 60°–110° with reference to the meridian. The rotation was assumed to be related to the right-lateral movement of the island arc along a north–south transform fault during the Paleogene. Two deformation stages were revealed for the central Olyutorsky Range and flysch complexes in its eastern part. The latter were deformed under post-Paleocene tectonic stresses applied from the Aleutian basin.

INTRODUCTION

The Olyutorsky Range is the eastern part of the Olyutorsky tectonic zone on the south of the Koryak highland (Fig. 1). Late Cretaceous, rarely Paleogene, island-arc and oceanic strata, as well as flysh complexes are common in the range [2, 3, 11, 13]. Its folded-nappe structure is sharply discordant relative to the other structural zones of the southern Koryak Highland.

Unlike the western areas of the Olyutorsky zone, the paleomagnetism of the Olyutorsky Range has been hardly researched; there has been only one paleomagnetic determination [9]. For this reason, our paleomagnetic studies were carried out over all of the structural–lithologic assemblages in the central range with the aim of drawing a comparison with available paleomagnetic data for the western Olyutorsky zone [4–6], to bring out relationships between the rocks involved in the structure of the range, and to refine current views on the structural evolution of the range and geodynamics of the region as a whole.

OBJECTS OF PALEOMAGNETIC STUDIES

These studies were carried out in the central range, in the head of the Vil'leikin River, in the Nichakvayam River basin, and more easterly, along the coast between Cape Witgenstein and the Ayat Lagoon (Fig. 1).

The lower part of the volcanogenic sequence, sampled in the Vil'leikin head is mostly composed of coarse tuffs and lava breccias with rare basaltic and basaltic andesite flows, and the upper part of this sequence contains an increased proportion of fine clastic rocks (Fig. 2). The presence of pyroclastics and geochemical data [2, 11] show that the sequence formed in an island-arc environment. Individual inoceramid findings indicate their age to be Campanian–Maastrichtian [11]. For paleomagnetic analysis, we sampled a sequence about 100 m thick, which mainly integrates members of fine and coarse clastic tuffs with single tuffaceous breccia horizons. The paleomagnetic samples were taken from fine clastic tuffs.

Both island-arc and oceanic volcanogenic sequences are exposed in the middle reaches of the Nichakvayam River [2, 11] (Fig. 3). Members of coarse clastic volcanogenic rocks with pillow basalt flows prevail in the basal island-arc strata. Up the sequence, the amount of coarse clastics decreases, and fine clastic tuffaceous rocks with pillow basalt intercalations become predominant The volcanogenic sequences in places are intruded by minor gabbro and dacite bodies. A relatively large layered dabbro block here shows tectonic contacts with surrounding deposits. The age of the island-arc sequences, based on radiolarians, is Campanian–Maastrichtian [2, 11].

The oceanic rocks are subdivided into "red" and "black" lava sequences [2, 11]. The former consists of basalts, hyaloclastites, and autoclastic breccias. Its radiolarian age is Santonian–Campanian [11]. The "red" lava sequence is a thick member of hematite-bearing sills and lavas so strongly dislocated, that the attitudes of numerous cshilled margins and of terrigenous rocks in sedimentary pockets are characterized by steep, nearly vertical dips slightly varying within the sequence. The age of the "red" sequence was tentatively accepted as Coniacian–Santonian [11]. The revealed sequences exhibit fault contacts. Paleomagnetic samples were taken from the upper island-arc section (sampled thickness is 250 m), from fine clastic volcanogenic rocks, and three blocks of the "red" lava sequence (chilled margins of sills and lava flows).

In the area located between the Witgenstein Cape and the Ayat Lagoon, flysch and olistostrome deposits

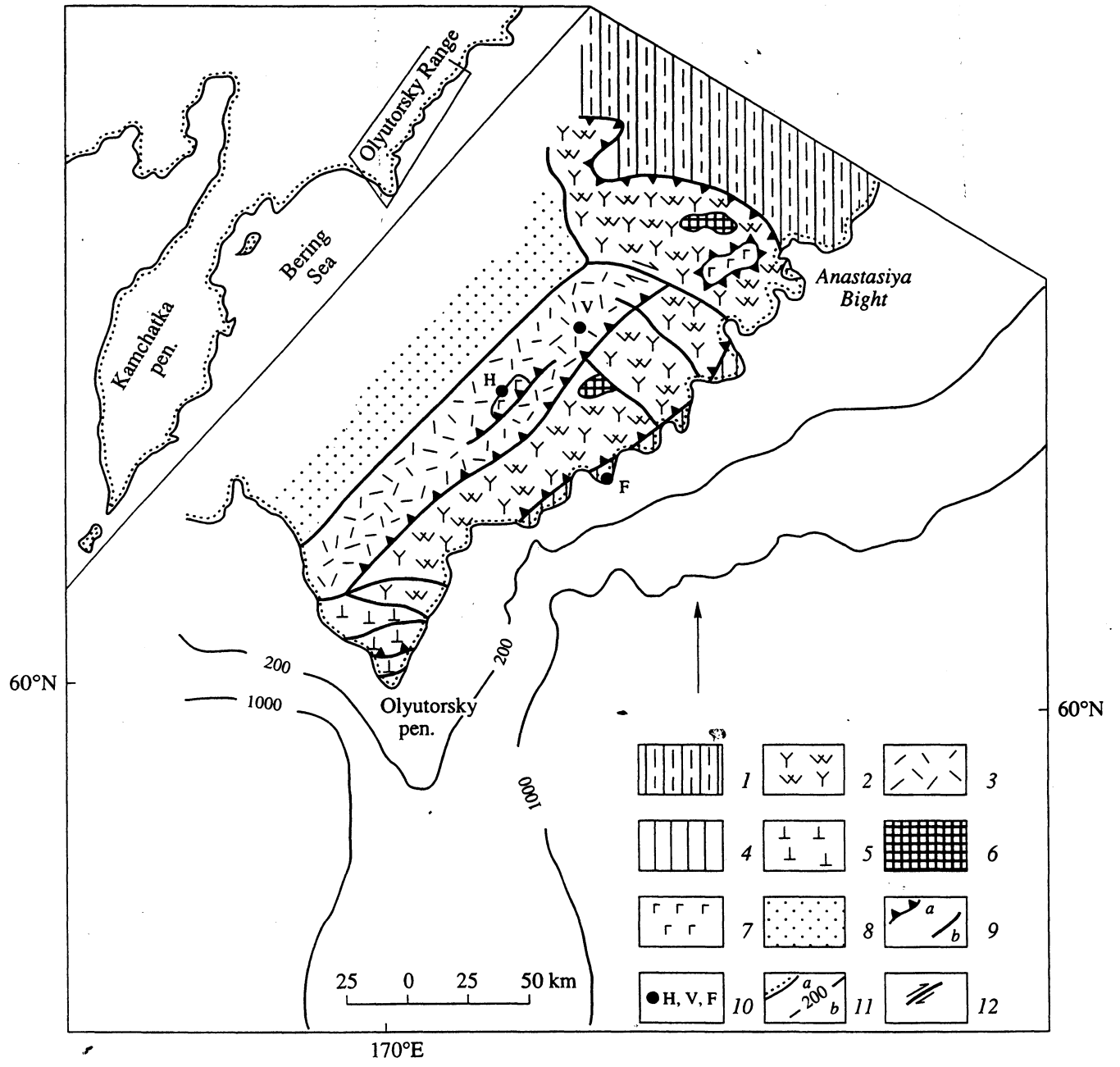

Fig. 1. Schematic structure of the Olyutorsky Range [13, 15]. (*1*) Flysch sequence of the Ukelayat Trough (K_2-Pg_1); (*2*) and (*3*) island-arc complexes: (*2*) siliceous and volcanic complex (K_2 San–K_2 Cmp), and (*3*) volcaniclastic complex (K_2 Cmp–K_2 Dan); (*4*) flysch–olistostrome sequence (K_2–Pg); (*5*) complex of oceanic alkaline basalts (K_2 Cmp–K_2 Dan); (*6*) relict (dunite–clinopyroxenite–gabbroic) complex (island-arc magma chambers); (*7*) oceanic basaltic complex (K_2 Alb–K_2 Tur); (*8*) volcanogenic–terrigenous complex, Apuka depression; (*9*) thrusts (*a*) and subvertical faults (*b*); (*10*) areas of field work in the Olyutorsky Range (H, Nichakvayam River; V, Vil'leikin River head; F, Cape Witgenstein); (*11*) coastline (*a*) and isobaths (*b*); (12) strike-slip faults. Contour in the inset outlines the Olyutorsky Range region.

were examined. The structural scheme of the area (Fig. 4) was composed by Chekhovich [13]. Two section types are recognized in these deposits. The first of them is distinguished by numerous olistoliths of cherts, oceanic basalts, and island-arc basalts. *In situ* flows of oceanic basalts chilled against the flysch deposits are also observed [13]. The second type of section is three-component flysch, which includes sandstones, siltstones, claystones, and no olistoliths. The flysch sequences of both types are intensely dislocated to form isoclinal folds and cleavaged. The cleavage and axial planes of the folds are consistently dipping to the northwest and north-northwest. The flysch and olistostrome sequences are overlain by low-angle southeast-dipping

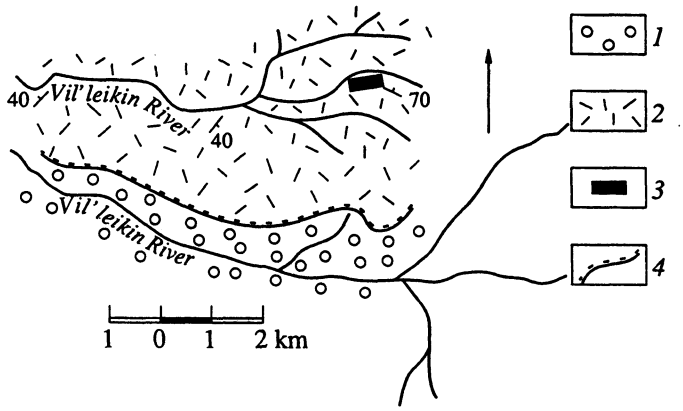

Fig. 2. Location of sampled area in the geological structure of the Vil'leikin River head waters. (*1*) Quaternary deposits; (*2*) island-arc volcaniclasfic complex (K_2 Maa–Dan); (*3*) sampled section; (*4*) geological boundaries.

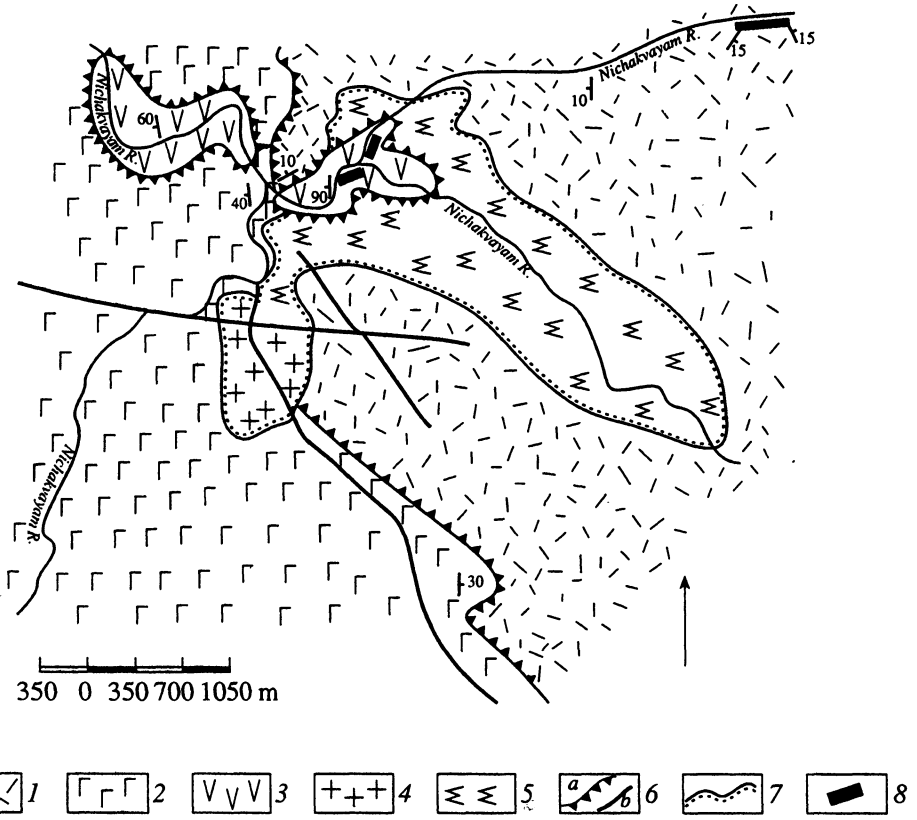

Fig. 3. Location of sampled areas in the geological structure of the middle reaches of the Nichakvayam River [14]. (*1*) Island-arc volcaniclastic rocks (K_2 Cmp–Dan); (*2*) and (*3*) oceanic sequences: (*2*) "black" lava sequence (K_2 San–Cmp) and (*3*) "red" lava sequence (K_2 Con–San); (*4*) subvolcanic dacite body; (*5*) layered gabbroic massif; (*6*) thrusts (*a*) and subvertical faults (*b*); (*7*) stratigraphic contacts and geological boundaries; (*8*) sites of paleomagnetic sampling.

nappes of siliceous rocks and volcanogenic sequences of island-arc origin. Relationships between the flysch sequences of the two types are unclear. According to V.S. Vishnevskaya, the radiolarian ages of many cherty olistoliths from type 1 flysch sequences are Santonian to Maastrichtian. The terrigenous matrix from both types of flysch sequences was dated by E.A. Shcherbinina on the basis of sporadic nannoplankton findings as Maastrichtian–Danian. Numerous radiolarian findings by Vishnevskaya from siliceous rocks overlying the flysch sequence in a thrust sheet yield Santonian–Danian ages. Farther to the south, in the area located between the Taman Lagoon and the Tamanvayam River basin, Paleocene–Early Eocene radiolarians were extracted from a member of silicified siltstone and claystone, which is tentatively referred to the flysch–olistostrome complex

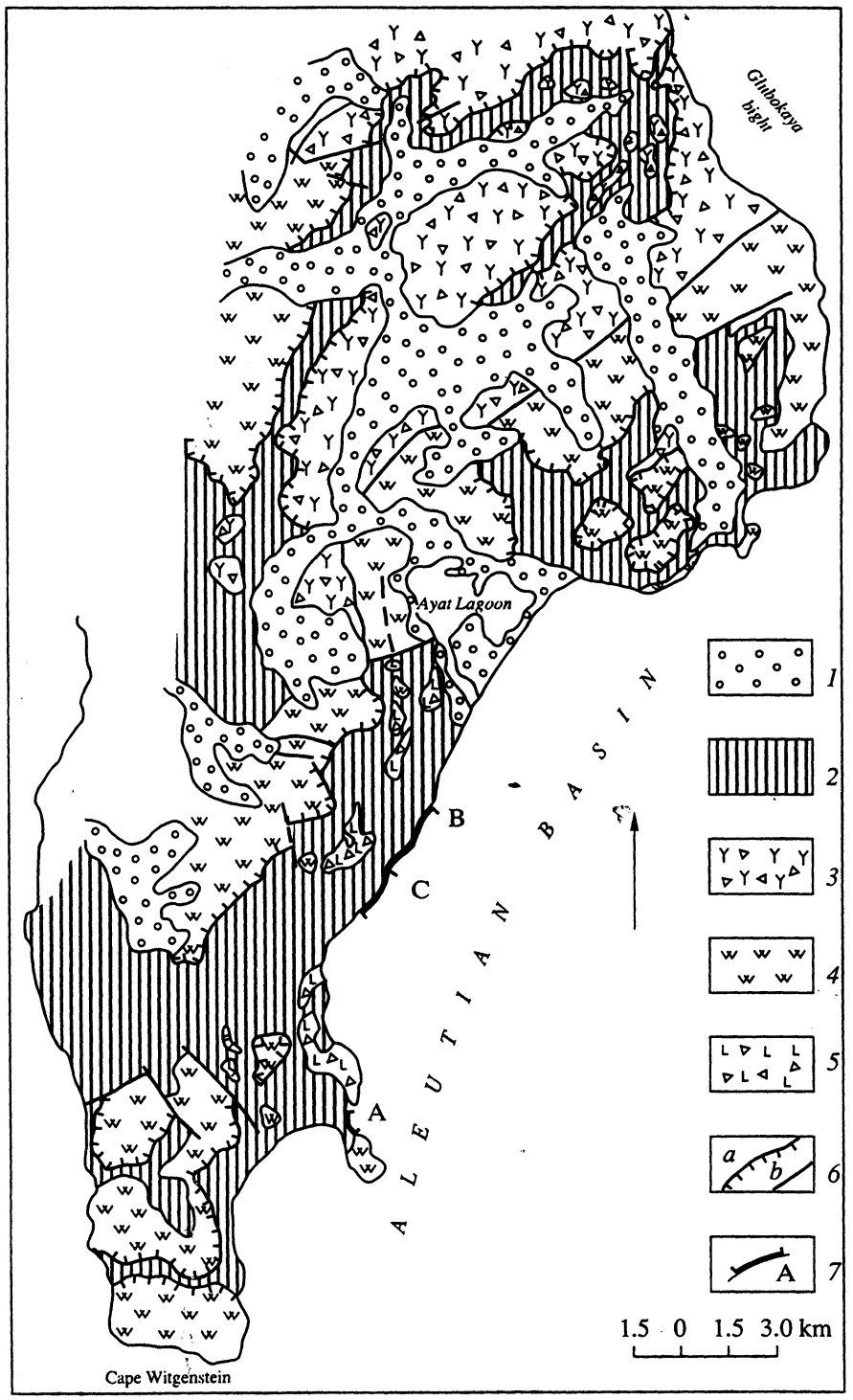

Fig. 4. Location of sampled areas in the Cape Witgenstein structure [15]. (*1*) Quaternary deposits; (*2*) Flysch–olistostrome sequence; (*3*) and (*4*) island-arc siliceous and volcanogenic complex: (*3*) alkali volcanites and volcanic breccias, (*4*) siliceous rocks (K_2 San–Cmp); (*5*) olistoliths and olistoplaques of oceanic basalts and hyaloclastites; (*6*) thrusts (*a*) and subvertical faults (*b*); (*7*) sites of paleomagnetic sampling A, B, and C.

[2]. Our paleomagnetic samples were collected from three least dislocated tectonic blocks of the flysch–olistostrome complex (fine sandstones, siltstones, and claystones); one block represents type 1 sequence, and the two others represent type 2 sequence.

TECHNIQUE OF LABORATORY PROCESSING OF PALEOMAGNETIC SAMPLES

Two or three cubes with 1- or 2-cm edges, depending on the magnitude of magnetic susceptibility, were

cut from each of the samples. The cubes were subject to heating within the temperature interval of 20 to 640°C, the upper boundary being determined by the temperature at which magnetic transformations distorting the natural remanent magnetization occurred. Most of the cubes were heated 10–12 times with a step of 50°C. The thermal cleaning was accomplished in a furnace placed in Helmholtz coils providing a compensation of the earth's magnetic field to 4–5 gamma. The remanent magnetization was measured with a JR-4 magnetometer. Data for each cubic specimen subjected to thermal cleaning were interpreted with the use of Zijderveld diagrams [22, 29], the paleomagnetic component analysis [22], and distribution of the revealed magnetization components on a sphere. The mean directions of these components were calculated for all the cubes of each sample. Some cubes were rejected, if their Zijderveld diagrams did not allow us to isolate any magnetic components (because of chaotic distributions of the directions, for example, owing to strong effects of magnetic transitions). Those specimens were also rejected for which none of the components could be calculated to obtain a mean direction with a confidence angle below 20°. A relatively high value of α_{95} was chosen because calculations for most of the samples were based on only two cubes. The directions of the distinguished components were analyzed on a sphere for each of the tectonic blocks and for all of the sampled blocks in the present-day (geographic) and ancient coordinate systems.

RESULTS OF MEASUREMENTS

The component analysis of samples from the volcanogenic sequence in the Vil'leikin River area showed a common presence of one or two magnetic components (Fig. 5, samples 223–240). The low-temperature components removable by heating to 300–350°C are directed in current geographic coordinates along the magnetic field of the Olyutorsky zone. The high-temperature components form a distinct group of vectors (Table 1), the mean direction of which does not coincide with the present direction of the geomagnetic field.

Magnetization of the "red" oceanic sill–lava sequence examined in the area of the Nichakvayam River (Fig. 5, samples 70, 85, and 90) is mainly represented by components of two types. The low-temperature components concordant to the present regional field are removed by heating to 250–300°C; the present components disappeared only in two samples heated to 500°C. The high-temperature components revealed in all three blocks form vector groups with mean directions whose statistical parameters are listed in Table 2 and illustrated in Fig. 6 (directions Isa, Isb, and Isc). These directions were found in both the magnetite and hematite temperature intervals (to 640°C, Table 2). The directions of the high-temperature magnetization components in all of the blocks differ from the present direction of the geomagnetic field in the region. The fold test [1] by means of comparing the mean directions (Table 2) and by the leveling method [12] (the ratio of the precision parameters in the geographic and stratigraphic coordinate systems is Kg/Ks = 2.1) argues for a considerable predominance of the postfold component.

The magnetization of samples from the island-arc Nichakvayam sequences is characterized by one or two components (samples 9–29, Fig. 5). The high-temperature components are clearly divided in two groups, one of which includes components of the normal polarity, and the other includes components of the reverse polarity (directions IhR and IhN, Figs. 6 and 7, Table 1). The low-temperature components are either close in direction to the present regional field, or are distributed chaotically. Irrespective of the polarity of the high-temperature components in these samples, the low-temperature components become extinct by heating to 250–300°C.

Distributions of the mean directions of magnetization, calculated from the high-temperature components of both the island-arc and oceanic sequences, show that the reverse IhR direction for the island-arc sequences coincides with the postfold magnetization direction in the oceanic "red" lava sequence (Fig. 6). Nevertheless, the formation of the IhR direction can hardly be related to processes that entailed remagnetization of the oceanic sequences, because their postfold magnetization is associated with hematite, and the magnetization of island-arc is rocks unstable above the magnetite Curie point.

None of the island-arc samples showed magnetization simultaneously caused by both the IhR and IhN high-temperature components (in an interval above at least 300°C); in other words, only one of these components is present in the samples. Therefore, these components are unlikely to be of different ages and superimposed as a result of remagnetization.

Microprobe analysis of many magnetic grains from the island-arc Nichakvayam and Vil'leikin samples with high-temperature magnetization components of the normal or reverse polarities showed that the samples contain titanomagnetites with the TiO_2 content ranging from 13 to 3%, and magnetite grains are rare (the grains to 3 μm were analyzed). Such a proportion of titanomagnetite and magnetite grains is typical of the primary distribution of these minerals in igneous island-arc rocks [15, 25]. Therefore, the island-arc complexes studied were not remagnetized by formation of secondary magnetite. The structure of the titanomagnetite grains is uniform, and although visible evidence of magnetic exsolution is absent, it is not inconceivable that fine magnetic exsolution of titanomagnetite undetected by microprobe could be present. The chemical compositions of titanomagnetites within individual grains are also homogeneous.

The reverse test, to compare the mean IhR and IhN directions for the Nichakvayam island-arc sequence,

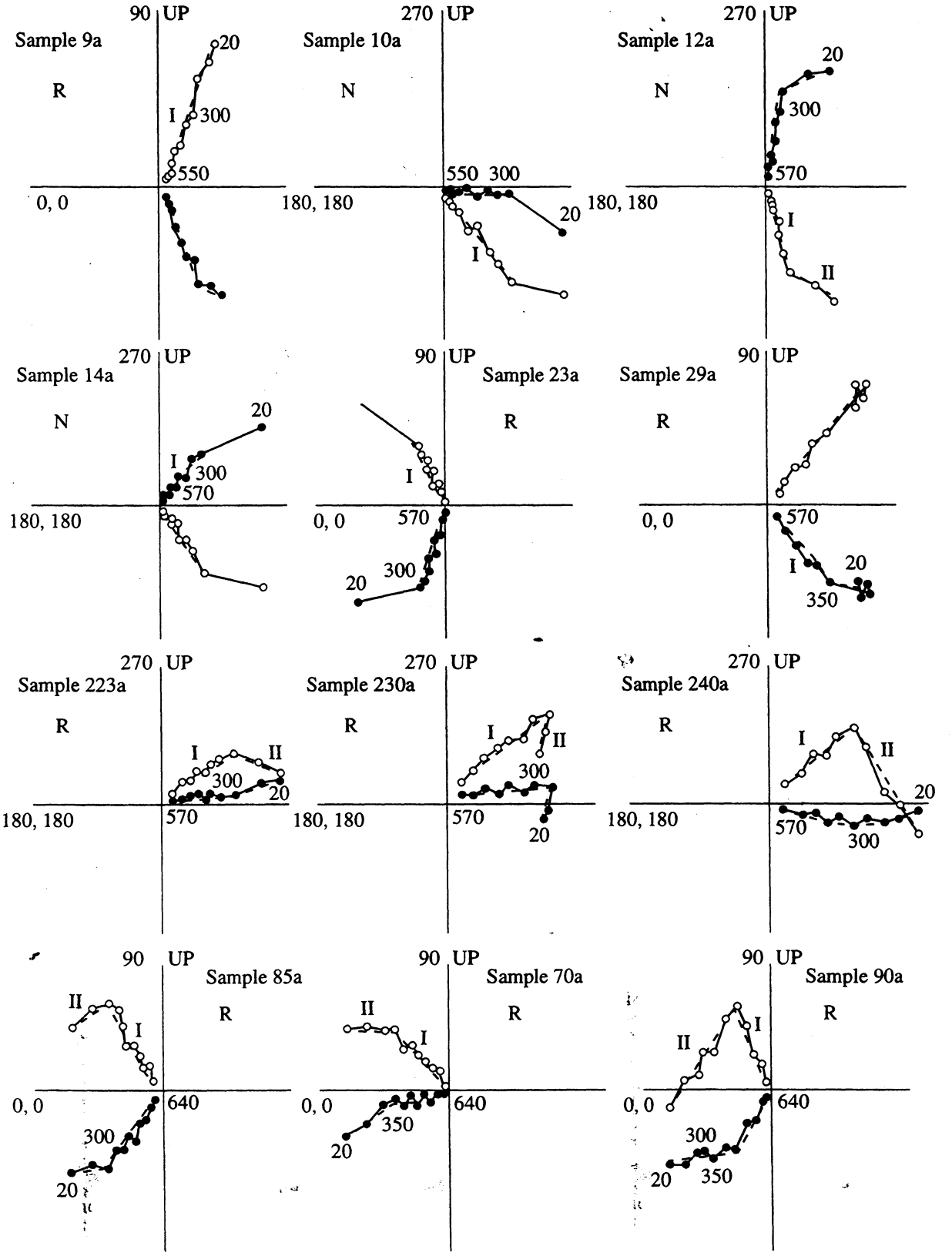

Fig. 5. Zijderveld's diagrams for rocks from the island-arc (samples 9–29 from the Nichakvayam River basin, and samples 223–240 from the Vil'leikin River head) and oceanic (samples 85–90 from the "red" lava sequence of the Nichakvayam River basin) sequences. The geographic coordinate system is used. Solid circles are projections of the magnetization vectors to the *xy* plane; open circles are their projections to the *xz* plane; the broken line is the revealed magnetization component; R and N are reverse and normal polarities of the high-temperature component, respectively; and I and II are numbers of the revealed components (Tables 1 and 2).

Table 1. Paleomagnetic data for the island-arc rock complex

N_1/N_0	Current coordinates				Past coordinates			
	D	I	K	α_{95}	D	I	K	α_{95}
Vil'leikin River head (v)								
Iv 17/15	9	–44	13	10	222	–72	12	10
IIv 17/5	354	64	12	18	5	–2	11	19
Nichakvayam River basin (h)								
Ih 28/22	80.4	78	15	8	80	66.5	13.6	8
IhR 28/8	278	–65	19	11	272	–56	28	9
IhN 28/14	38	84	18	9	66	72	13	10
IIh 28/6	244	83	5	25	54	84	7	22
Mean for all sections (v, h)								
Ih, Iv 37	164	72	6	9	67	70	12	6
IhN, Iv 29	184	68	6	10	54	72	13	7
Fold test (comparison of mean directions)								
IhR, IhN	$f_2 = 0.3528$				$f_2 = 0.2184$		$f^{cr} = 0.2334$	
Iv, Ih	$f_2 = 1.24$				$f_2 = 0.095$		$f^{cr} = 0.116$	
IhN, Iv	$f_2 = 1.14$				$f_2 = 0.0255$		$f^{cr} = 0.117$	

Note: I and II, high- and low-temperature components, respectively; N and R, normal and reverse polarities, respectively; v and h, strata indices; N_1/N_0, the ratio of the number of samples taken from exposures to that used in calculations; D, declination; I, inclination; K, precision parameter; α_{95}, radius of confidence range; f and f^{cr}, calculated and critical values of Fisher's distribution, respectively [1].

Table 2. Paleomagnetic data for the oceanic complex rocks

N_1/N_0	Current coordinates				Past coordinates			
	D	I	K	α_{95}	D	I	K	α_{95}
"Red" oceanic lava sequence (s), Nichakvayam River								
Isa 20/19	322	–55	31	6	80	–35	15	8
Isb 4/4	333	–52	14	18	70	–13	14	18
Isc 6/6	305	–66	17	14	117	–34	17	14
Mean for all blocks (a, b, c)								
Is 30/29	321	–57	22	5.5	86	–33	10	8
Isg 30/27	306	–60	11	8	97	–35	7	10
IIs 30/15	353	66	16	9	313	–8	16	9
Fold test (comparing the mean directions)								
Isa, Isb, Isc	$f_3 = 2.06$				$f_3 = 7.06$	$f^{cr}_{(4, 52, 0.05)} = 2.35$		
Isa + Isb, Isc	$f_2 = 0.087$				$f_2 = 0.337$	$f^{cr} = 0.117$		
Is, Isg	$f_2 = 0.038$				$f_2 = 0.025$	$f^{cr} = 0.057$		

Note: I and II, high- and low-temperature components, respectively; s, strata index; a, b, and c, block indices; Isg, magnetization direction calculated from segments of Zijderveld diagrams in the hematite temperature interval (580 to 640°C). For other indices, see Table 1.

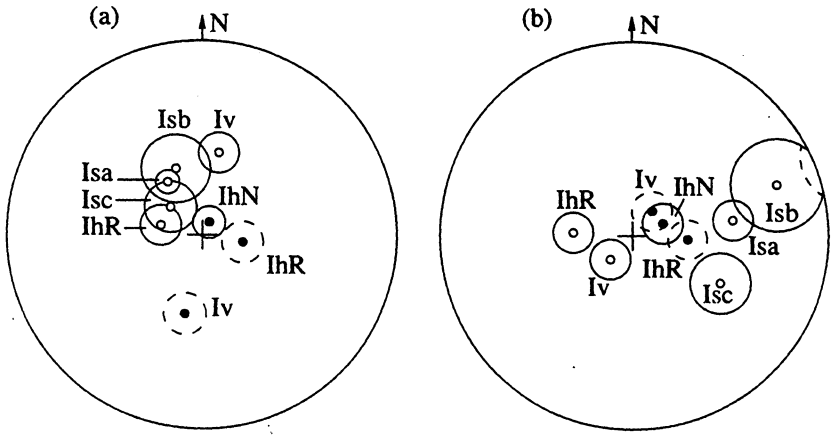

Fig. 6. Stereograms of the mean magnetization directions in the island-arc and oceanic sequences with the confidence ranges. (a) Current coordinate system and (b) age coordinate system. Solid and open centers mark directions of normal and reverse polarities, respectively. Dashed circles are for directions of magnetization converted from the reverse to the normal polarity. Letter symbols are explained in Tables 1 and 2.

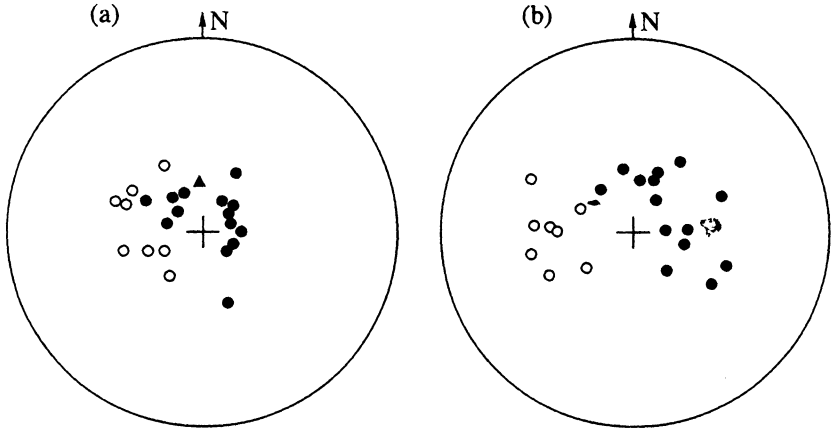

Fig. 7. Stereograms of the high-temperature magnetization components in rocks from the island-arc sequences of the Nichakvayam River basin. (a) Current coordinate system and (b) age coordinate system. Solid and open centers mark directions of normal and reverse polarities respectively. Dashed circles are for directions of magnetization, and the triangle is the present regional direction of the geomagnetic field.

showed that these directions, when transformed to the normal polarity, are statistically identical in the past coordinate system, but are different in the current geographic coordinates (Table 1).

The fold test, carried out by the same method with Iv direction determined from the coeval island-arc rocks of the Vil'leikin River, is positive in the past coordinate system and negative in the current coordinates (Fig. 6, Table 1). Hence it follows that the revealed directions are likely to be of the prefold origin. Note that folding in the central Olyutorsky Range is assumed to be of Eocene age.

Thus, the positive fold and reversal tests and results of microprobe analysis allow the IhR and IhN directions to be treated as coeval (within the estimated age range of the sequences) directions of different polarity (Fig. 7, Table 1). The same data showed that all of the high-temperature magnetization components in the island-arc complexes are of the prefolding stage and may be related to the primary magnetization.

The component analysis, applied to samples from the flysch sequences in the area of the Witgenstein Cape and the Ayat Inlet, revealed the complex character of magnetization. Their Zijderveld diagrams indicate one-, two-, and three-component magnetization (samples 150–154, block B; samples 161–165, block C; and samples 209–221, block A). Each of the components distinguished in the sampled tectonic blocks forms two relatively distinct groups of vectors of normal polarity in the geographic coordinate system (directions marked by roman digits II and III, respectively). Furthermore, magnetization of some samples consists of two components, which are distributed between two groups, and the magnetization of the other samples is represented only by one component falling into any one of the groups. The mean direction of the vectors in group III for all these blocks coincides with the present field

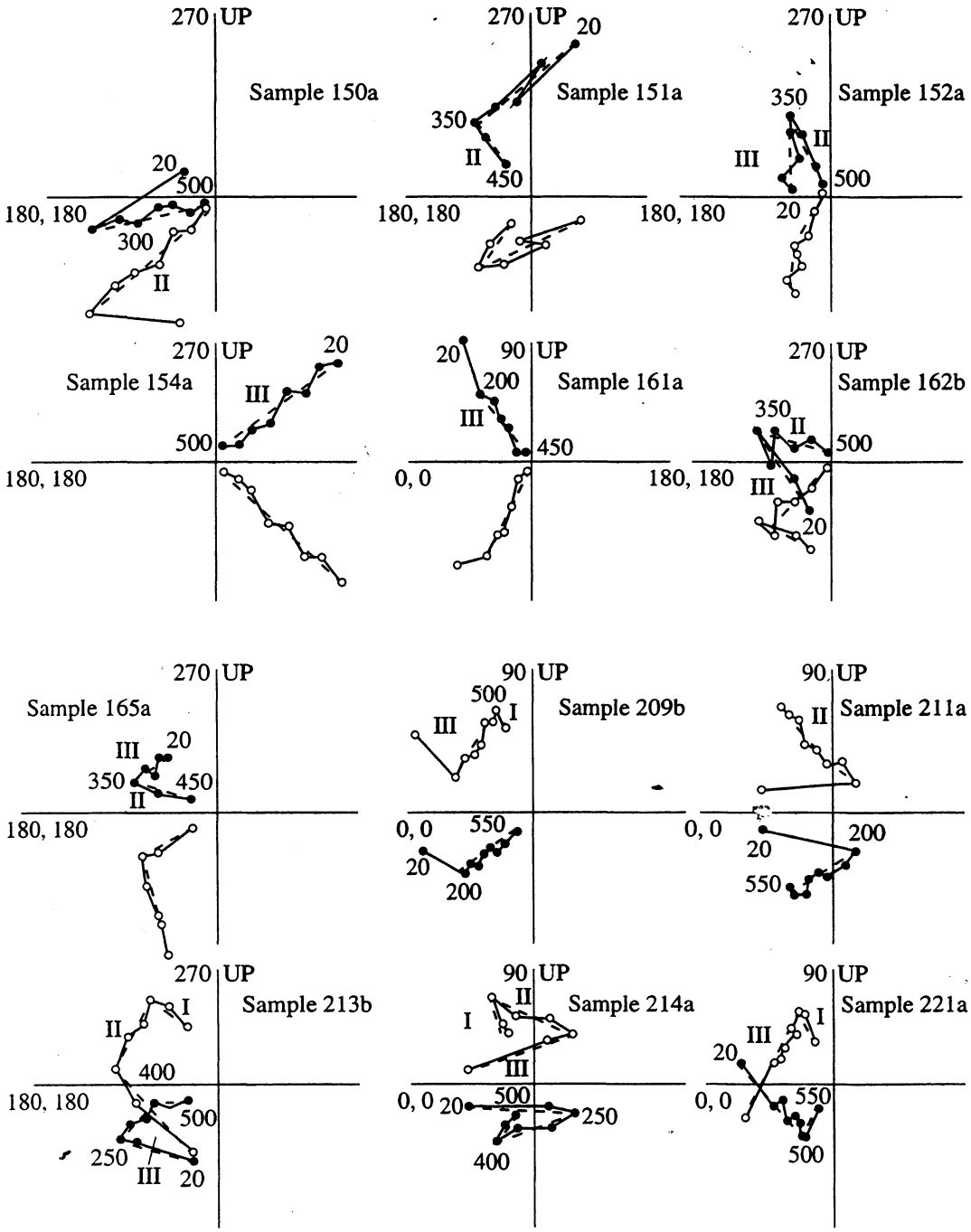

Fig. 8. Zijderveld diagrams for samples from the flysch–olistostrome complex (samples 150–154, block B; samples 161–165, block C; samples 209–221, block A). The current coordinate system is used. Solid circles are projections of magnetization vectors to the *xy* plane, and open circles are their projections to the *xz* plane. The broken line is the revealed magnetization components. I, II, and III are the numbers of these components (Table 3).

direction in the region, and the mean direction of the vectors in group II differs from it. Note that the components of group III show the lowest, and those of group II higher temperature.

We succeeded in revealing group III of magnetization vectors with the reverse polarity (direction IA, Table 3) in block A (type 1 sequence). Their direction was calculated at the highest temperature points in Zijderveld diagrams, which do not approach the origin of coordinates, and from the highest temperature components, distinguished in some two- and three-component Zijderveld diagrams, where they are approaching the origin of coordinates (Fig. 8, samples 209b, 213b, 214a, and 221a). The calculations are based only on

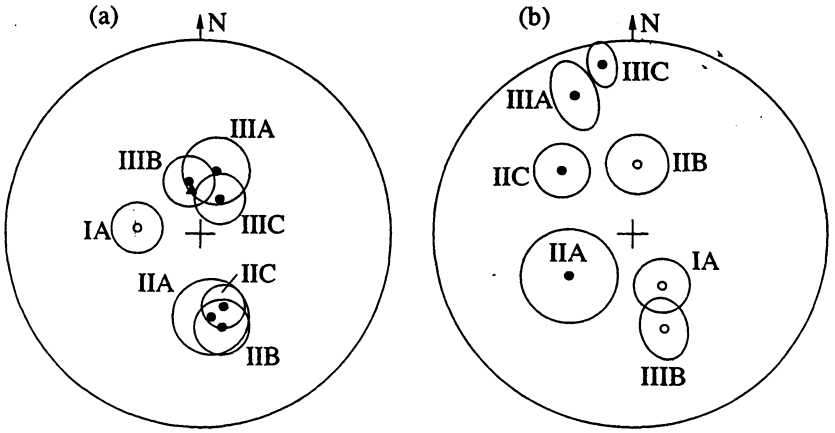

Fig. 9. Stereograms of the mean magnetization directions with confidence ranges for the flysch–olistostrome sequence in (a) current and (b) past coordinate systems. For explanation, see Table 3.

directions providing satisfactory convergence of results for two cubic specimens ($\alpha_{95} < 20°$).

The fold test for mean II and III directions in all the blocks clearly shows that both are of the postfold origin (Table 3, Fig. 9).

Any test for IA direction within the flysch complex is impossible, because the direction was calculated in only one block with slight variations in bedding attitude. Nevertheless, we may hypothesize this direction to be the most ancient, possibly predated folding. This assumption is based on the fact that this direction is the highest in temperature parameter sharply differs from the present regional field direction in the current coordinate system, has an inclination close to that in the coeval island-arc Vil'leikin and Nichakvayam com-

Table 3. Paleomagnetic data for rocks of the flysch complex

N_1/N_0		Current coordinates				Ancient coordinates			
		D	I	K	α_{95}	D	I	K	α_{95}
Block A (type I flysch)									
IA	19/13	280	–64	10	12	157	–65	12	11
IIA	19/9	176	55	7	18	238	57	4	22
IIIA	19/6	19	64	14	15	339	26	11	17
After rotation for 40° southward									
IARt		219	–48	10	12				
After straightening by recalculated attitude									
IAAN		219	–48	10	12	169	–65	12	11
Block B (flysch II)									
IIB	17/11	171	50	11	12	5	–62	8	14
IIIB	17/11	355	68	13	12	165	–46	13	12
Block C (type II flysch)									
IIC	22/14	167	57	19	8	312	51	11	11
IIIC	22/9	36	73	21	10	350	15	12	13
Mean for all blocks (A, B, and C)									
IIA, B, C	34	171	54	12	7	311	32	2	19
IIIA, B, C	26	14	70	14	7	348	–26	1	24
Fold test (comparing the mean directions)									
IIA, B, C		$f_3 = 0.361$			$f_3 = 40.3$			$f^{cr}_{(4, 62, 0.05)} = 2.35$	
IIIA, B, C		$f_3 = 1.41$			$f_3 = 68.1$			$f^{cr}_{(4, 46, 0.05)} = 2.35$	

Note: A, B, and C, indices of blocks; IARt, IA direction recalculated to the position of the flysch–olistostrome complex turned for 40° southward; IAAN, IA direction given in the ancient coordinate system according to attitude of beds in the block A if the flysch–olistostrome complex is rotated for 40° southward. For other notes see Table 1.

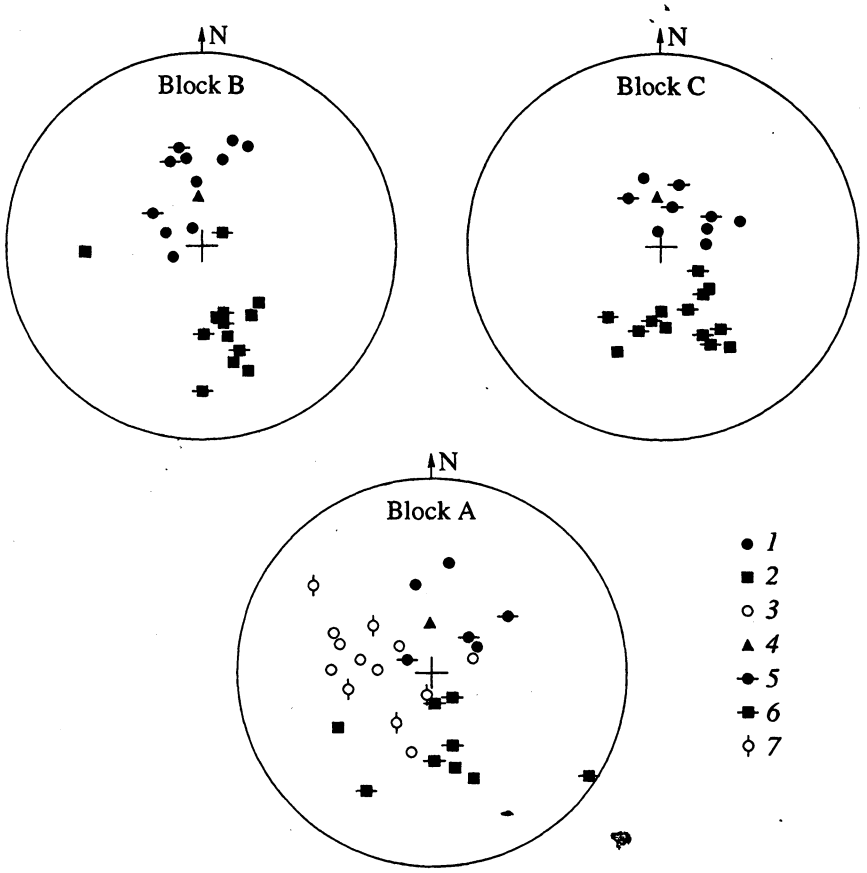

Fig. 10. Stereograms of the magnetization components revealed in three blocks of the flysch–olistostrome complex. (*1*) Component III, (*2*) component II, and (*3*) component I (see Table 3), (*4*) the present field direction in the Olyutorsky Range region. Dashed solid circles and squares are the only magnetization components in sample. Dashed open circles are the components distinguished by the highest temperature segments of Zijderveld diagrams, which tend to the origin of coordinates, and open circles are the components calculated with the use of one highest temperature point in the Zijderveld diagram.

plexes in the ancient coordinate system, and is different from them in the geographic coordinate system.

INTERPRETATION OF RESULTS

(1) The formative latitude of the Campanian-Maastrichtian island-arc complexes of the Olyutorsky Range (the Olyutorsky–Karaginsky island arc [6]), calculated from the mean inclination of the revealed magnetization ranges from 45° to 63°N, the average latitude being 53°N. These data are consistent with paleomagnetic results for Late Cretaceous island-arc sequences in the other areas of the Olyutorsky zone [4–6, 9]. The estimated interval of formative latitude for the type 1 flysch sequence is 35°–63°N, the average latitude being 47°N, but this result, based on the assumption that IA direction is of prefold origin is less certain because of the large angle of confidence.

(2) Comparison of the paleolatitudes, obtained for the island-arc complexes in the central Olyutorsky Range, with the expected paleolatitudes, i.e., those calculated for the coordinates of the region from the Cretaceous and Paleocene–Eocene paleomagnetic poles of Eurasia and North America showed that these complexes cannot be aligned with either Eurasia, or North America for the time interval between the end of the Cretaceous and the beginning of the Paleogene. Our calculations were made following Beck's [16] method and allowed for Demarest's correction [18]. It was found that F = 13 and $\Delta F = 7.5$ (using the Late Cretaceous pole [28]), and F = 12.6 and $\Delta F = 5.3$ (using the Paleocene–Eocene pole [28]) for the Eurasian continent, and F = 11 and $\Delta F = 5.7$ (using the Late Cretaceous pole [28]), and F = 10.5 and $\Delta F = 5.6$ (using the Paleocene–Eocene pole [28]) for the North American continent. The significant differences in paleolatitude between the Olyutorsky–Karaginsky island arc and the Eurasian and North American continents in the Late Cretaceous–Early Paleocene are estimated to have been 500 and 700 km respectively. The same distances, calculated from the average latitudes, are 2000 and 2200 km, respectively.

Comparison of the paleolatitudes calculated for the island-arc complexes of the Olyutorsky Range with the paleolatitudes available for the Late Cretaceous molasse Koryak complexes, 64°–76°–90°N (the upper

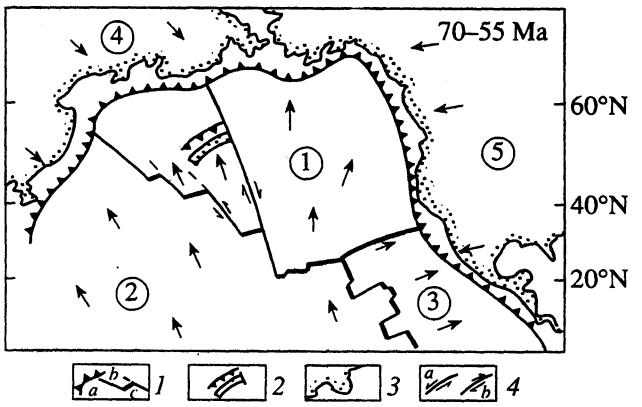

Fig. 11. Hypothetical reconstruction of motion of the Olyutorsky–Karaginsky island arc during the Maastrichtian and Paleocene. (*1*) Plate boundaries: (*a*) subduction, (*b*) transform, (*c*) spreading; (*2*) Olyutorsky–Karaginsky island arc; (*3*) continental contours; (*4*) motions along transform faults: (*a*) left-lateral and (*b*) right-lateral. Figures in the scheme: 1—Kula plate; 2—Pacific plate; 3—Farallon plate; 4—Eurasian plate; and 5—North American plate. Arrows indicate plate motions. Kinematic data were taken from papers by Kirschvink [22] and Rubenstone [24].

limit, average value, and lower limit, respectively) [19], and for Alaska, 59°–67°–76°N [27], also show that the Olyutorsky–Karaginsky island arc was at an appreciable distance from the central Koryakia and Alaska during the Late Cretaceous and Early Paleocene.

(3) The island-arc sequences in the central Olyutorsky Range rotated clockwise for the angle of 60°–100° around the vertical axis, relative to the meridian. The significant angles of rotation relative to North America and Eurasia, calculated by Beck's method with the use of the Late Cretaceous and Paleocene–Eocene poles for these continents, are 37°–39° (R = 59° and ΔR = 22° assuming the Late Cretaceous pole [28], and R = 60° and ΔR = 20° assuming the Paleocene–Eocene pole [28]) and 34°–50° (R = 77° and ΔR = 43° assuming the Late Cretaceous pole [28], and R = 71° and ΔR = 20° assuming the Paleocene–Eocene pole [28]), respectively. The rotation of at least the Nichakvayam island-arc sequences is unrelated to the deformation caused by formation of the nappe-folded structure of the Olyutorsky Range, because these strata are almost undistorted.

Table 4. Expected magnetization vectors calculated for the Olyutorsky Range using data on the Cretaceous and Cenozoic, Eurasian and North American paleomagnetic poles

Age	Paleolatitude	D	I	α_{95}
		Eurasia		
K_2	74.8	349	82	6.8
Pg_1–Pg_2	74	355	82	1.6
Pg_3	72.5	340	81	7.4
Ng_1	70	355	79.5	3.7
Ng_2	67	355.5	78	1.6
		North America		
65 Ma	72.5	7.6	81	3.1
K_2	75.8	16	83	4
Pg_1–Pg_2	70	4.5	79	2.6
Pg_3	66.4	359	77	2.2
Ng_1	64	357	76	2.2
Ng_2	62.3	1	75.3	1.7

(4) The oceanic sequences exposed in the Nichakvayam River area underwent at least two deformation stages. The first of them took place prior to formation of the detected postfold component, and the second stage occurred after the formation of this component and resulted in its deviation from the direction of the earth's field in which the sequence was remagnetized (Fig. 6). It may be hypothesized that the oceanic and island-arc sequences rotated about the vertical axis as a result of a single tectonic process because the declinations of both the postfold magnetization of the oceanic complex and the prefold magnetization of the island-arc complex substantially deviate clockwise relative to the meridian (Fig. 6).

(5) Table 4 lists the expected declinations for Eurasia and North America, calculated using data on the Cretaceous and Tertiary paleomagnetic poles of these continents for the Olyutorsky Range coordinates [16, 28]. Obviously, the maximum rotation angle of Eurasia and North America in a clockwise direction since the Cretaceous to the present is only 15° (the rotation occurred during a period from the Oligocene to the Pliocene), and North America rotated slightly anticlockwise during the same time interval. Therefore, the calculated angles of clockwise rotation for the blocks in the Olyutorsky Range cannot be explained by their rotation along with the continents after their collision with the island arc.

It is hardly probable that the rotation of the blocks was related to the assumed northwest-directed Cenozoic spreading in the Aleutian basin [17] because its slip component relative to the continental margin is very small, and the spreading direction could be responsible only for anticlockwise rotation of the blocks (Figs. 11 and 12).

More acceptable is a hypothesis that the block rotation of the Olyutorsky Range is related to the right-lateral movement of the Olyutorsky–Karaginsky island arc along a transform fault bordering it on the east and extending north–south along the Shirshov Ridge (Fig. 11). The Paleocene is the most probable time of this movement, because it was the period during which both the Kula and Pacific plates moved northward [20, 23], and, early in the Eocene, the study regions were sheltered from the Pacific plates by the Aleutian arc and proto-Komandorsky strike-slip fault [5] (Fig. 12). The assumption that the Olyutorsky–Karaginsky island arc was separated from the Pacific plates is based on the chilled contacts between *in situ* preorogenic oceanic basalts and the middle Eocene flysch of Karaginskiy

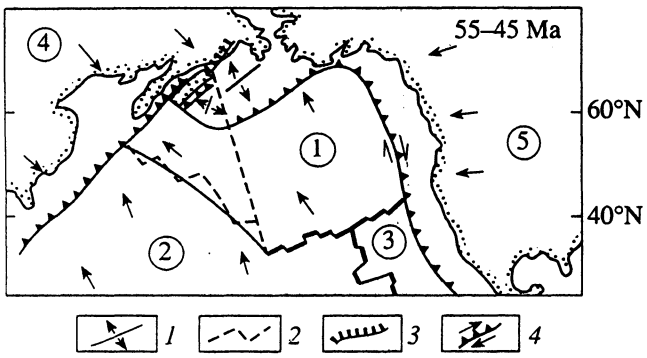

Fig. 12. Reconstructed position of the Olyutorsky–Karaginsky island arc in the Eocene. (*1*) Spreading direction, (*2*) boundaries of the Pacific lithospheric plates prior to change in the spreading direction in the Kula Ridge, (*3*) vergence of the thrust-and-fold structures; and (*4*) subduction zones with the slip component of the subducting plates. For other symbols see Fig. 11.

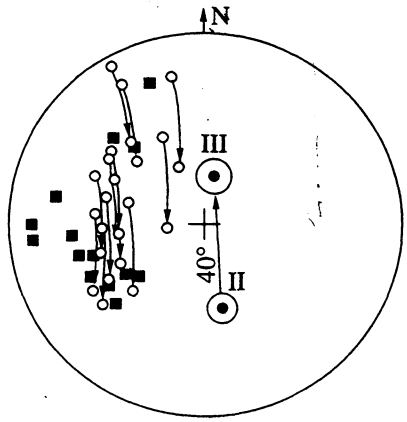

Fig. 13. Stereogram of the normals to cleavage planes and axial planes of folds (circles) before and after (indicated by arrows) the 40° rotation of the flysch–olistostrome complex in the southerly direction. Solid squares are the dip directions of these planes after the rotation of the structure.

Island [7, 14]. Therefore, a back-arc spreading took place in the Komandorsky Basin as early as the middle Eocene. The spreading direction in the Kula Ridge also changed to northwestern at the Paleocene–Eocene boundary [23], resulting in separation of the Olyutorsky–Karaginsky island arc from the Pacific plates.

(6) The fact that the two postfold components were revealed in all the sampled blocks of flysch–olistostrome sequences in the area of Cape Witgenstein and the Ayat Lagoon suggests that these sequences experienced at least two deformation stages. The isoclinally folded flysch structure formed during stage 1, and during stage 2, the already deformed sequences were turned over for about 40° (a significant interval between the postfold directions) northward (Fig. 13). The opposite, southward, rotation of the structure, to the point of coincidence of the second postfold component with the present geomagnetic field direction in the region, shows the vergence of the structure prior to this deformation stage. Figure 13 shows the position of the normals to some measured axial planes of isoclinal folds and to the cleavage planes before and after the rotation of the structure. It is clear that the vergence of the structure before the second deformation stage was more easterly.

(7) The northward vergence of the structure might be related to tectonic movements directed from the Aleutian Basin of the Bering Sea. This conclusion confirms an assumption made by Cooper *et al.* [17], on back-arc spreading within the Aleutian Basin during the Paleogene. Deformation in the northern direction was also observed in more northerly regions of the western rim of the Aleutian Basin [10].

(8) The island-arc and oceanic blocks in the central Olyutorsky Range rotated clockwise, and the declinations of both postfold components distinguished in the flysch–olistostrome complex coincide with the meridian. Hence it follows that formation of both these components and tilting of the flysch structure toward the north occurred after the rotation of the blocks, most likely, after the Paleocene. This assumption is supported by the presence of the Eocene flysch strata in the fold-and-thrust structure of the Olyutorsky Range (Taman Inlet). The direction of folding in the flysch–olistostrome sequence at the first stage (eastern and east-northeastern vergence) is coincident with that of deformation in the central Olyutorsky Range. This folding is most likely to have occurred in the first half of the Eocene, since the upper age limit of 45 m.y. [21] for formation of the nappe-folded structure of the range is derived from the age of intrusive rocks of the Machevna Massif cutting through the nappe-folded sequence. The overthrusting stage that led to formation of the nappes correlates with the formation stage of the Koryak nappes northwest of the Olyutorsky Range [8, 10]. This overthrusting may be related either to tectonic stresses that acted before inception of the Aleutian subduction zone [24, 26], or to an important stage of back-arc spreading in the Aleutian basin. The second stage of overturning of some fragments on the eastern coast of the Olyutorsky Range is most likely to have been associated with a new spreading stage in the Aleutian Basin (Fig. 12).

CONCLUSIONS

(1) The paleolatitude interval of formation of the Campanian–Maastrichtian island-arc complexes in the Olyutorsky Range is 45°–53°–63°N (minimum, average, and maximum values, respectively).

(2) The island-arc complexes studied cannot be aligned with Eurasia, or with North America for the time interval between the end of the Cretaceous and the beginning of the Paleogene.

(3) The oceanic sequences exposed in the Nichakvayam River area have gone through at least two deformation stages.

(4) The island-arc and oceanic sequences studied rotated clockwise around the vertical axis for 60°–110° relative to the meridian. The rotation angles with respect to North America and Eurasia are 37°–39° and 34°–50°, respectively. It is assumed that the rotation of these sequences is unrelated to folding during formation of the nappe-folded structure of the Olyutorsky Range and was caused by movements along a north–south transform fault during the Paleocene.

(5) The flysch sequences in the area of Cape Witgenstein and the Ayat Lagoon are likely to have experienced two deformation stages. The isoclinally folded, eastward-vergent flysch structure formed during the first stage, and, during the second stage (probably, after the Paleocene), the entire structure was overturned for 40° northward. Such overturning might have been caused by tectonic movements directed from the Aleutian Basin.

ACKNOWLEDGMENTS

This work was supported by the Russian Foundation for Basic Research (project no. 94-05-17300) and the Nadezhda Foundation.

I am grateful to the researchers of the Borok Geophysical Observatory for permission to use their paleomagnetic apparatus, to M.I. Il'in for assistance in microprobe measurements, and N.A. Bogdanov, V.D. Chekhovich, and other researchers from the Department of the Oceanic Crust, Institute of the Lithosphere, Russian Academy of Science, for helpful discussion of the materials presented.

REFERENCES

1. Bazhenov, M.L. and Shipunov, S.V., The Fold Test in Paleomagnetism, *Izv. Akad. Nauk SSSR, Fiz. Zemli,* 1988, no. 7, pp. 89–101.
2. Bogdanov, N.A., Vishnevskaya, V.S., Kepezhinskas, P.K., Sukhov, A.N., and Fedorchuk, A.V., *Geologiya yuga Koryakskogo nagor'ya* (Geology of the Southern Koryak Highland), Moscow: Nauka, 1987.
3. Bogdanov, N.A., Chekhovich, V.D., Sukhov, A.N., and Vishnevskaya, V.S., Tectonics of the Olyutorsky Zone, in *Ocherki tektoniki Koryakskogo nagor'ya* (Sketches on Tectonics of the Koryak Highland), Moscow: Nauka, 1982, pp. 189–217.
4. Kovalenko, D.V., Paleomagnetic Studies of Island-Arc Complexes in the Olyutorsky Zone and Karaginsky Island and Tectonic Interpretation of Results, *Geotektonika,* 1990, no. 2, pp. 92–101.
5. Kovalenko, D.V., Paleomagnetism of the Paleogene Complexes in the Il'pinskii Peninsula (Geological Interpretation), *Geotektonika,* 1992, no. 5, pp. 78–95.
6. Kovalenko, D.V., Paleomagnetism of the Paleogene Complexes in the Il'pinskii Peninsula (Physical Bases of the Method), *Fiz. Zemli,* 1993, no. 5, pp. 72–80.
7. Kravchenko-Berezhnoy, I.R., Geological Position of Igneous Complexes in the Western Rim of the Kommandorsky Basin, *Cand. Sci. (Geol.-Mineral.) Dissertation,* Moscow: Institute of the Lithosphere, Russian Academy of Sciences, 1989.
8. Ruzhentsev, S.V., Byalobzheskii, S.G., Grigor'ev, V.N., Kazimirov, A.D., Peive, A.A., and Sokolov, S.D., Tectonics of the Koryak Range, in *Ocherki tektoniki Koryakskogo nagor'ya* (Sketches on Tectonics of the Koryak Highland), Moscow: Nauka, 1992, pp. 136–188.
9. Savostin, L.A. and Kheifets, A.N., Paleomagnetism of the Maastrichtian–Lower Paleocene Island-Arc Formations in the Olyutorsky Zone (Southern Koryak Area), in *Paleomagnetizm i akkretsionnaya tektonika* (Paleomagnetism and Accretionary Tectonics), Leningrad: Vses. Nauch. Issl. Geologorazved. Inst., 1988, pp. 127–140.
10. Sokolov, S.D., *Akkretsionnaya tektonika Koryakskogo–Kamchatskogo segmenta Tikhookeanskogo poyasa* (Accretionary Tectonics of the Koryak–Kamchatka Segment of the Pacific Belt), Moscow: Nauka, 1992.
11. Fedorchuk, A.V., Geology of Siliceous and Volcanogenic Formations of the Olyutorsky Range, *Cand. Sci. (Geol.-Mineral.) Dissertation,* Moscow: Institute of the Lithosphere, Russian Academy of Sciences, 1985.
12. Khramov, A.N., Goncharov, G.I., Komissarova, R.A., Pisarevskii, V.V., and Gurevich, E.M., *Paleomagnitologiya* (Paleomagnetology), Leningrad: Nedra, 1982.
13. Chekhovich, V.D., Geology and Geodynamic Environments of Formation of the Preorogenic Frame of Minor Oceanic Basins, *Doctoral (Geol-Mineral.) Dissertation,* Moscow: Institute of the Lithosphere, Russian Academy of Sciences, 1989.
14. Chekhovich, V.D., Bogdanov, N.A., Kravchenko-Berezhnoy, I.R., Averina, G.Yu., Gladenkov, A.Yu., and Til'man, S.M., *Geologiya zapadnoi chasti Beringova morya* (Geology of the Western Bering Sea), Moscow: Nauka, 1990.
15. Arculus, R.J. and Will, K.J.A., The Petrology of Plutonic Blocks and Inclusions from Lesser Antilles Island Arc, *J. Petrol.,* 1980, vol. 21, no. 4, pp. 743–799.
16. Beck, M.E., Jr., Paleomagnetic Record of Plate-Margin Tectonic Processes Along the Western Edge of North America, *J. Geophys. Res.,* 1980, vol. 85, pp. 7115–7131.
17. Cooper, A.K., Marlow, M.S., Scholl, D.W., and Steveson, A.J., Evidence for Cenozoic Crustal Extension in the Bering Sea Region, *Tectonics,* 1992, vol. 11, no. 4, pp. 719–731.
18. Demarest, H.H., Jr., Error Analysis for the Determination of Tectonic Rotation from Paleomagnetic Data, *J. Geophys. Res.,* 1983, vol. 88, pp. 4321–4328.
19. Didenko, A.N., Harbert, W., and Stavskiy, A.W., Paleomagnetism of Khatyrka and Mayniscky Superterranes, *Tectonophysics,* 1993, vol. 220, no. 9, pp. 141–155.
20. Engebretson, D.C., Cox, A., and Gordon, R.C., Relative Motions between Oceanic Plates of the Pacific Basin, *J. Geophys. Res.,* 1984, vol. 89, pp. 291–310.
21. Kepezhinskas, P.K., Reuber, I., Tanaka, H., and Miyashita, S., Zoned Calc–Alkaline Plutons in Northeastern Kamchatka, Russia: Implications for the Crustal Growth in Magmatic Areas, *Mineral. Petrol.,* 1993, vol. 49, pp. 147–174.

2. Kirschvink, J.L., The Least-Squares Line and Plane and the Analysis of Paleomagnetic Data, *Geophys. J. R. Astron. Soc.*, 1980, vol. 62, pp. 699–718.

3. Lonsdale, P., Paleogene History of the Kula Plate: Offshore Evidence and Onshore Implications, *Geol. Soc. Am. Bull.*, 1988, vol. 100, no. 5, pp. 733–754.

4. Rubenstone, J.L., Geology and Geochemistry of Early Submarine Volcanic Rocks of the Aleutian Islands and Their Bearing on the Development of the Aleutian Island Arc, *Doctoral (Ph.D.) Dissertation*, Ithaca, N.Y.: Cornell University, 1984.

5. Scarfe, C.M. and Toshitsugu, F., Petrology of Crystal Clots in the Pumice of Mount St. Helen's March 19, 1982 Eruption: Significant Role of Fe–Ti Oxide Crystallization, *J. Volcanol. Geothermal. Res.*, 1987, vol. 34, no. 1/2, pp. 1–14.

26. Scholl, D.W., Vallier, T.L., and Stevenson, A.J., Terrane Accretion, Production, and Continental Growth: A Perspective Based on the Origin and Tectonic Fate of the Aleutian–Bering Sea Region, *Geology*, 1986, vol. 14, no. 1, pp. 43–47.

27. Stone, D.B., Paleogeography and Rotations of Arctic Alaska—an Unresolved Problem, *Paleomagnetic Rotations and Continental Deformation*, Kissel, C. and Laj, C., Eds., Kluwer, 1989, pp. 343–364.

28. Westphal, M., Bazhenov, M.L., Lauer, J.P., *et al.*, Paleomagnetic Implications on the Evolution of the Tethys Belt from the Atlantic Ocean to Pamirs since the Triassic, *Tectonophysics*, 1986, vol. 123, pp. 37–82.

29. Zijderveld, J.D.A., A.C. Demagnetization in Rocks: Analysis of Results, *Methods in Paleomagnetism*, Collinson, P.W., Creer, K.M., and Runcorn, S.K., Eds., New York: Elsevier, 1967, pp. 254–286.